Amplitude Variation with Offsets and Azimuths Simultaneous Inversion for Elastic and Fracture Parameters

Zhaoyun Zong*, Xingyao Yin and Guochen Wu

China University of Petroleum, Qingdao, Shandong, China

Abstract: Azimuthal elastic inversion or AVO/AVA analysis has proven to be effective for fracture description and stress evaluation in unconventional resource plays. Fracture weakness including normal and tangential weakness from linear slip theory bridge the seismic data and fracturing parameters as intermediate parameters. However, the stability of the azimuthal elastic inversion methods available for anisotropic parameters or fracture parameters in field data remains challenging. This study explores a practical azimuthal simultaneous elastic inversion method in heterogeneous medium for fracture weakness estimation. Taking the heterogeneity and anisotropy of fracture media into consideration, and based on perturbation theory and stable phase approximation, the fracture medium can be considered as the superimposition of background medium and perturbation medium, and then the seismic scattering coefficient of fracture media can be derived. This equation establishes the relationship between seismic data and fracture weakness together with elastic parameters like P-wave and S-wave moduli and weaknesses. With this equation, a heterogeneous inversion method is proposed. This method implements the estimation of P-wave and S-wave moduli and fracture weaknesses simultaneously, and the constraint from initial model and multi-iterations enhances the stability of this method. In this approach, the parameters of the perturbation medium are initially estimated, and then they can be superposed to the parameters of the known background medium as the renewal parameters of the background medium in next iteration. We can yield the final estimation of the parameters in heterogeneous medium after several iterations when the last two estimated results are similar. Model test and field data examples verify the feasibility and potential of the proposed approach.

Keywords: AVAZ, Fracture weaknesses, Seismic scattering coefficient, Stable phase approximation.

1. INTRODUCTION

Under the hypothesis of aligned fractures system, the fracture analysis with P-wave seismic data has been studied a lot in literature. Conventionally, three kinds of models are utilized for the characterization of aligned fractured reservoirs, including linear-slip model in terms of dimensionless quantities normal weakness Δ_N and tangential weakness Δ_T for rotationally invariant fractures [1], isolated parallel penny-shaped cracks [2-3] and partially saturated penny-shaped cracks or hydraulically connected cracks and pores [4]. Details of different theories and models of cracked media and their interconnectivity can be found in Bakulin *et al.* [5].

The variation of kinetic parameter like P-wave velocity [6-11] or dynamical parameter like seismic amplitude variations with offset or incident angle and azimuth (AVOZ/AVAZ) [12-22] is usually applied in fracture analysis and further study like fluid discrimination or stress evaluation. However, compared with seismic velocities, the reflection amplitudes own higher resolution and are more sensitive to reservoirs [23-24]. AVOZ/AVAZ analysis and AVOZ/AVAZ inversion are mainly two ways to study a single fracture system. The former is utilized usually for fracture orientation and fracture density prediction with the ellipse fitting method, and the latter aims at estimating the anisotropic parameters directly with different effective medium theories.

One of the important factors in AVOZ/AVAZ analysis or inversion is the knowledge of reflection coefficient when P-wave impinges on a horizontal interface separating two media of varying elastic stiffness. The analytical expression or approximations for P-wave reflection coefficients of different anisotropic media have been studied a lot. Stress-displacement eigenvector matrices were utilized in calculation of reflection coefficients numerically in Fryer and Frazer [25]. Thomsen [26] proposed the concept of weak anisotropy which facilitated the derivation of different reflectivity approximations for anisotropic media. The first-order perturbation approach was conventionally utilized in deriving reflectivity coefficients [27-28] . The approximate reflection coefficients of P-wave for interfaces separating two HTI was initially introduced by Ruger. However, this approximation is impossible to tell whether the anisotropic gradient is positive or negative, which will introduce a 90 degree ambiguity into the estimation of fracture orientation as shown in Downton *et al.* [20]. To avoid the tedious sequence of algebraic exercises resulting from first-order perturbation of the exact reflection coefficients of anisotropic media, Shaw and Shaw [29] introduced an approach to derive the approximation of exact reflection coefficients incorporating Born approximation and stationary phase hypothesis and also utilized the Born formalism to derive the sensitivity to fracture

*Address correspondence to this author at the China University of Petroleum, Qingdao, Shandong, China; Tel: +86 15165267370; Fax: +86 0532 86981879; E-mail: zhaoyunzong@yahoo.com

E-ISSN: 2409-787X/14

weakness of PP- and PS-reflection coefficients for an interface separating an unfractured medium from a vertically fractured medium in terms of normal weakness Δ_N and tangential weakness Δ_T [30]. They also explored the inversion approach to estimate the fluid indicator for a simple layered horizontal model. However, the influence of wavelets was not considered in their inversion approach, and they also discussed less about the stability of the approach in field data. In addition, Downton and Roure [20] introduced a simultaneous elastic inversion method to estimate elastic parameters, normal weakness Δ_N and tangential weakness Δ_T with the exact P-wave reflection coefficient equation. However, they also discussed less about the stability of the inversion algorithm. To extend the application of azimuthal simultaneous elastic inversion in field data, we proposed a practical amplitude variation with incident angle and azimuth (AVAZ) inversion approach for fracture weakness estimation. The seismic scattering coefficient equation in terms of P-wave modulus, S-wave modulus, density, normal weakness Δ_N and tangential weakness Δ_T of HTI media is firstly derived combining Born approximation and stationary phase hypothesis. Furthermore, we develop a robust inversion approach to estimate these parameters with the seismic scattering coefficient equation in Bayesian scheme. The constraint from initial model and multi-iterations enhances the stability of this method. Model test and field examples verify the feasibility of the proposed method and we also explore the application of this method in the stress evolution in a field data example.

2. MODEL PARAMETERIZATION OF HTI MEDIA WITH ELASTIC MODULI AND FRACTURE WEAKNESSES

For heterogeneous anisotropic elastic media, the constitutive matrix $\mathbf{C}$ can be expressed as,

$$\mathbf{C} = \mathbf{C}_0 + \Delta\mathbf{C}_{iso} + \Delta\mathbf{C}_{ani} \tag{1}$$

Where $\mathbf{C}_0$ is the constitutive matrix of homogeneous background media, $\mathbf{C}_{\text{iso}}$ is the constitutive matrix of homogeneous perturbation media and $\mathbf{C}_{ani}$ is the constitutive matrix of anisotropic perturbation media.

Specifically for aligned fractures system (HTI media), we can parameterize the heterogeneous media in terms of P-wave modulus M, S-wave modulus μ, fracture normal weakness Δ_N and fracture tangential weakness Δ_T as,

$$\mathbf{C} = \mathbf{C}_0 + \Delta\mathbf{C}_{iso} + \Delta\mathbf{C}_{HTI}$$

Where

$$\mathbf{C}_0 = \begin{bmatrix} M_0 & M_0-2\mu_0 & M_0-2\mu_0 & 0 & 0 & 0 \\ M_0-2\mu_0 & M_0 & M_0-2\mu_0 & 0 & 0 & 0 \\ M_0-2\mu_0 & M_0-2\mu_0 & M_0 & 0 & 0 & 0 \\ 0 & 0 & 0 & \mu_0 & 0 & 0 \\ 0 & 0 & 0 & 0 & \mu_0 & 0 \\ 0 & 0 & 0 & 0 & 0 & \mu_0 \end{bmatrix} \tag{2}$$

$$\Delta\boldsymbol{C}_{iso} = \begin{bmatrix} \Delta M & \Delta M-2\Delta\mu & \Delta M-2\Delta\mu & 0 & 0 & 0 \\ \Delta M-2\Delta\mu & \Delta M & \Delta M-2\Delta\mu & 0 & 0 & 0 \\ \Delta M-2\Delta\mu & \Delta M-2\Delta\mu & \Delta M & 0 & 0 & 0 \\ 0 & 0 & 0 & \Delta\mu & 0 & 0 \\ 0 & 0 & 0 & 0 & \Delta\mu & 0 \\ 0 & 0 & 0 & 0 & 0 & \Delta\mu \end{bmatrix} \tag{3}$$

And,

$$\Delta\boldsymbol{C}_{HTI} = -M_0 \begin{bmatrix} \Delta_N & (1-2\eta)\Delta_N & (1-2\eta)\Delta_N & 0 & 0 & 0 \\ (1-2\eta)\Delta_N & (1-2\eta)^2\Delta_N & (1-2\eta)^2\Delta_N & 0 & 0 & 0 \\ (1-2\eta)\Delta_N & (1-2\eta)^2\Delta_N & (1-2\eta)^2\Delta_N & 0 & 0 & 0 \\ 0 & 0 & 0 & 0 & 0 & 0 \\ 0 & 0 & 0 & 0 & \eta\Delta_T & 0 \\ 0 & 0 & 0 & 0 & 0 & \eta\Delta_T \end{bmatrix} \tag{4}$$

Where $\eta = \mu_0 / M_0$, M_0 and μ_0 is the P-wave modulus and S-wave modulus of the homogeneous background media, respectively.

3. SEISMIC WAVE SCATTERING COEFFICIENT OF HTI MEDIA

Under the hypothesis of weak scattering, the scattering wave field of heterogeneous HTI media in frequency domain can be expressed as [31],

$$\boldsymbol{u}^s(\boldsymbol{x}',\omega) = \int_V \begin{pmatrix} \omega^2\Delta\rho(\boldsymbol{x}^s)u_i^0(\boldsymbol{x}^s,\omega)G_{ni}^0(\boldsymbol{x}^s,\omega;\boldsymbol{x}') \\ -\Delta c_{ijkl}(\boldsymbol{x}')\dfrac{\partial u_k^0(\boldsymbol{x}^s,\omega)}{\partial x_l}\dfrac{\partial G_{ni}^0(\boldsymbol{x}^s,\omega;\boldsymbol{x}')}{\partial x_j} \end{pmatrix} d\boldsymbol{x}^s \tag{5}$$

Where u^0 is the wave field of the background homogeneous media, ω is circular frequency, $u_i^0(\bullet)$ and $G_{ni}^0(\bullet)$ is the elastic wave field of excitation source and Green function, respectively. $G_{ni}^0(\boldsymbol{x}^s,\omega;\boldsymbol{x}')$ is the wave field at receiver $\boldsymbol{x}'$ inspired from source $\boldsymbol{x}^s$. $\Delta\rho = \rho - \rho_0$ is the difference between the density of heterogeneous media ρ and the density of background

homogeneous media ρ_0. Δc_{ijkl} is the superposition of elastic stiffness of perturbation homogeneous media (Equation (3)) and perturbation HTI media (Equation (4)). ΔM and $\Delta\mu$ is the P-wave modulus and S-wave modulus of perturbation homogeneous media, respectively.

The elastic wave field $u_{mi}\left(\boldsymbol{x}',\omega\right)$ at $\boldsymbol{x}'$ inspired from $\boldsymbol{x}^s$ is,

$$u_{mi}\left(\boldsymbol{x}',\omega\right)=G_{mi}\left(\boldsymbol{x}^s,\omega;\boldsymbol{x}'\right) \tag{6}$$

The Green function of point source can be defined as,

$$\boldsymbol{G}\left(\boldsymbol{r},\omega\right)=\frac{N_n N_i}{4\pi\rho_0\alpha_0^2}\frac{1}{\boldsymbol{r}}e^{i\omega r/\alpha_0} \tag{7}$$

Where N_n and N_i are the source and receiver direction, respectively. α_0 is the P-wave velocity of homogeneous background media. $\boldsymbol{r}$ is the distance between the source and receiver.

Substituting equation (6) and (7) into equation (5) yields,

$$\begin{aligned}&\boldsymbol{u}^s\left(\boldsymbol{r},\omega\right)=N_m M_n\omega^2\int_V d\boldsymbol{r}\left[\left(\Delta\rho\delta_{ik}+\Delta c_{ijkl}s_j^s s_l\right)p_i^s p_k\right]\\&A\left(\boldsymbol{r}\right)e^{i\omega\varphi\left(\boldsymbol{r}\right)}\end{aligned} \tag{8}$$

Where $\boldsymbol{s}$ and $\boldsymbol{s}^s$ are the slowness vector of incident wave and scattering wave, respectively. $\boldsymbol{p}$ and $\boldsymbol{p}^s$ are the polarization vector of incident wave and scattering wave, respectively. N_m is the projection of source direction to incident ray path, and M_n is the projection of receiver direction to scattering ray path. $\varphi\left(\boldsymbol{r}\right)$ is the phase after scattering, and $A\left(\boldsymbol{r}\right)$ is the amplitude,

$$A\left(\boldsymbol{r}\right)=\frac{1}{\left(4\pi\rho_0\alpha_0^2\right)^2}\frac{1}{\boldsymbol{r}^2} \tag{9}$$

With equation (8) and (9), we can see that the amplitude of the scattering wave in far field varies slowly. However, the phase of the scattering wave in far field varies large and rapid oscillations. With stationary phase approximation, the P-wave scattering displacement at $\boldsymbol{r}=\boldsymbol{r}_0$ is,

$$\begin{aligned}&\boldsymbol{u}^s\left(\boldsymbol{r},\omega\right)=-N_m M_n\frac{1}{4\pi\rho_0\alpha_0^2\boldsymbol{r}_0}\\&\left(\frac{1}{4\rho_0\cos^2\theta}\left(\Delta\rho\delta_{ik}+\Delta c_{ijkl}s_j^s s_l\right)p_i^s p_k\mid_{r=r_0}\right)e^{i\omega\varphi\left(r_0\right)}\end{aligned} \tag{10}$$

substituting equation (10) and (7) yields,

$$R_S\left(\theta,\phi\right)=\frac{1}{4\rho_0\cos^2\theta}\left(\Delta\rho\delta_{ik}+\Delta c_{ijkl}s_j^s s_l\right)p_i^s p_k\mid_{r=r_0} \tag{11}$$

Where $R_S\left(\theta,\phi\right)$ is the P-wave scattering coefficient. With equation (3) and equation (4) yields,

$$\begin{aligned}&R_S\left(\theta,\phi\right)=\left(\frac{1}{2}-\frac{1}{4}\frac{1}{\cos^2\theta}\right)\frac{\Delta\rho}{\rho_0}+\frac{1}{4}\frac{1}{\cos^2\theta}\frac{\Delta M}{M_0}\\&-2\frac{\mu_0}{M_0}\sin^2\theta\frac{\Delta\mu}{\mu_0}-\frac{1}{4}\sec^2\theta\left(1-2\eta+2\eta\sin^2\theta\cos^2\phi\right)^2\\&\Delta_N-\eta\tan^2\theta\cos^2\phi\left(\sin^2\theta\sin^2\phi-\cos^2\theta\right)\Delta_T\end{aligned} \tag{12}$$

Where θ is the incident angle, ϕ is the difference between azimuth of survey line and fracture direction. ΔM, $\Delta\mu$ and $\Delta\rho$ is the homogeneous perturbation. As follows, we will present a practical inversion method in Bayesian scheme with model constraint to estimate the P-wave modulus, S-wave modulus, density, normal weakness and tangential weakness in HTI media.

4. ESTIMATION OF THE PARAMETERS IN HETEROGENEOUS FRACTURED MEDIA

With equation (12), we can estimate the P-wave modulus, S-wave modulus, density, normal weakness and tangential weakness in HTI media with model constraint in Bayesian scheme as follows. To enhance the stability, equation (12) can be rearranged as,

$$\begin{aligned}&R_S\left(\theta,\phi\right)=a\left(\theta\right)L_\rho+b\left(\theta\right)L_M+c\left(\theta\right)L_\mu\\&+d\left(\theta,\phi\right)\Delta_N+e\left(\theta,\phi\right)\Delta_T\end{aligned} \tag{13}$$

Where $L_\rho=\frac{\Delta\rho}{\rho_0}$, $L_M=\frac{\Delta M}{M_0}$, $L_\mu=\frac{\Delta\mu}{M_0}$

$$a\left(\theta\right)=\left(\frac{1}{2}-\frac{1}{4}\frac{1}{\cos^2\theta}\right) \tag{14}$$

$$b\left(\theta\right)=\frac{1}{4\cos^2\theta} \tag{15}$$

$$c\left(\theta\right)=-2\sin^2\theta \tag{16}$$

$$d\left(\theta,\phi\right)=-\frac{1}{4}\sec^2\theta\left(1-2\eta+2\eta\sin^2\theta\cos^2\phi\right)^2 \tag{17}$$

$$e\left(\theta,\phi\right)=-\eta\tan^2\theta\cos^2\phi\left(\sin^2\theta\sin^2\phi-\cos^2\theta\right) \tag{18}$$

When there are three subsurface interfaces and two azimuths, equation (13) can be expressed in matrix form as,

$$\begin{bmatrix} {}_1r_1^1 \\ {}_1r_1^2 \\ {}_1r_1^3 \\ {}_1r_2^1 \\ {}_1r_2^2 \\ {}_1r_2^3 \\ {}_2r_1^1 \\ {}_2r_1^2 \\ {}_2r_1^3 \\ {}_2r_2^1 \\ {}_2r_2^2 \\ {}_2r_2^3 \end{bmatrix} = \begin{bmatrix} a_1^1 & 0 & 0 & b_1^1 & 0 & 0 & c_1^1 & 0 & 0 & d_1^1 & 0 & 0 & e_1^1 & 0 & 0 \\ 0 & a_1^1 & 0 & 0 & b_1^1 & 0 & 0 & c_1^1 & 0 & 0 & d_1^1 & 0 & 0 & e_1^1 & 0 \\ 0 & 0 & a_1^1 & 0 & 0 & b_1^1 & 0 & 0 & c_1^1 & 0 & 0 & d_1^1 & 0 & 0 & e_1^1 \\ a_2^1 & 0 & 0 & b_2^1 & 0 & 0 & c_2^1 & 0 & 0 & d_2^1 & 0 & 0 & e_2^1 & 0 & 0 \\ 0 & a_2^1 & 0 & 0 & b_2^1 & 0 & 0 & c_2^1 & 0 & 0 & d_2^1 & 0 & 0 & e_2^1 & 0 \\ 0 & 0 & a_2^1 & 0 & 0 & b_2^1 & 0 & 0 & c_2^1 & 0 & 0 & d_2^1 & 0 & 0 & e_2^1 \\ a_1^2 & 0 & 0 & b_1^2 & 0 & 0 & c_1^2 & 0 & 0 & d_1^2 & 0 & 0 & e_1^2 & 0 & 0 \\ 0 & a_1^2 & 0 & 0 & b_1^2 & 0 & 0 & c_1^2 & 0 & 0 & d_1^2 & 0 & 0 & e_1^2 & 0 \\ 0 & 0 & a_1^2 & 0 & 0 & b_1^2 & 0 & 0 & c_1^2 & 0 & 0 & d_1^2 & 0 & 0 & e_1^2 \\ a_2^2 & 0 & 0 & b_2^2 & 0 & 0 & c_2^2 & 0 & 0 & d_2^2 & 0 & 0 & e_2^2 & 0 & 0 \\ 0 & a_2^2 & 0 & 0 & b_2^2 & 0 & 0 & c_2^2 & 0 & 0 & d_2^2 & 0 & 0 & e_2^2 & 0 \\ 0 & 0 & a_2^2 & 0 & 0 & b_2^2 & 0 & 0 & c_2^2 & 0 & 0 & d_2^2 & 0 & 0 & e_2^2 \end{bmatrix} \begin{bmatrix} L_M^1 \\ L_M^2 \\ L_M^3 \\ L_\mu^1 \\ L_\mu^2 \\ L_\mu^3 \\ L_\rho^1 \\ L_\rho^2 \\ L_\rho^3 \\ \Delta_N^1 \\ \Delta_N^2 \\ \Delta_N^3 \\ \Delta_T^1 \\ \Delta_T^2 \\ \Delta_T^3 \end{bmatrix} \quad (19)$$

Considering the influence of wavelets in different incident angle and azimuth, equation (19) can be expressed in general matrix form as,

$$\mathbf{D} = \mathbf{G} \cdot \mathbf{L} \quad (20)$$

Where $\mathbf{G}$ is wavelet matrix incorporating coefficient matrix. $\mathbf{L}$ is the parameters to be estimated.

Incorporating the prior information in Bayesian inversion scheme [32-35], the maximum posteriori probability is,

$$F(\boldsymbol{L}) = (\boldsymbol{D} - \boldsymbol{GL})^{\mathrm{T}}(\boldsymbol{D} - \boldsymbol{GL}) + 2\sigma_n^{\,2}\sum_{i=1}^{k}\ln(1 + \boldsymbol{L}_i^2 / \sigma_m^2) \quad (21)$$

Where $\sigma_n^{\,2}$ is the variance of noise. σ_m^2 is the variance of parameters to be estimated. k is the number of parameters to be estimated.

Incorporating the initial model constraint into the initial objective function (21), the final objective function becomes,

$$\begin{aligned} F(\boldsymbol{L}) &= (\boldsymbol{D} - \boldsymbol{GL})^{\mathrm{T}}(\boldsymbol{D} - \boldsymbol{GL}) + 2\sigma_n^{\,2}\sum_{i=1}^{k}\ln(1 + \boldsymbol{L}_i^2 / \sigma_m^2) \\ &+ \lambda_{\boldsymbol{M}}(\eta_{\boldsymbol{M}} - \mathrm{P}\ \boldsymbol{M}_r)^T(\eta_{\boldsymbol{M}} - \mathrm{P}\ \boldsymbol{M}_r) + \lambda_\mu(\eta_\mu - \mathrm{P}\ \mu_r)^T(\eta_\mu - \mathrm{P}\ \mu_r) \\ &+ \lambda_{\boldsymbol{D}}(\eta_{\boldsymbol{D}} - \mathrm{P}\ \boldsymbol{D}_r)^T(\eta_{\boldsymbol{D}} - \mathrm{P}\ \boldsymbol{D}_r) + \lambda_{\boldsymbol{N}}(\eta_{\boldsymbol{N}} - \mathrm{P}\ \boldsymbol{N}_r)^T(\eta_{\boldsymbol{N}} - \mathrm{P}\ \boldsymbol{N}_r) \\ &+ \lambda_{\boldsymbol{T}}(\eta_{\boldsymbol{T}} - \mathrm{P}\ \boldsymbol{N}_r)^T(\eta_{\boldsymbol{T}} - \mathrm{P}\ \boldsymbol{N}_r) \end{aligned} \quad (22)$$

Where, $\lambda_{\boldsymbol{M}}, \lambda_\mu, \lambda_{\boldsymbol{D}}, \lambda_{\boldsymbol{N}}, \lambda_{\boldsymbol{T}}$ is the constraint coefficient for P-wave modulus, S-wave modulus, density, and normal weakness and tangential weakness, respectively. P is $\int_{t_0}^{t} d\tau$, and,

$$\eta_{\mathbf{M}} = \frac{1}{2}\ln(\mathbf{M} / M_0) \quad (23)$$

$$\eta_\mu = 1/2 * \ln(\boldsymbol{\mu} / \mu_0) \quad (24)$$

$$\eta_{\mathbf{r}} = 1/2 * \ln(\mathbf{D} / D_0)\,. \quad (25)$$

$$\eta_{\mathbf{N}} = \Delta_N\,. \quad (26)$$

$$\eta_{\mathbf{T}} = \Delta_T\,. \quad (27)$$

Where, M_0, μ_0 and D_0 is the initial P-wave modulus, S-wave modulus and density, which can be estimated from log curves. Incorporating singular value

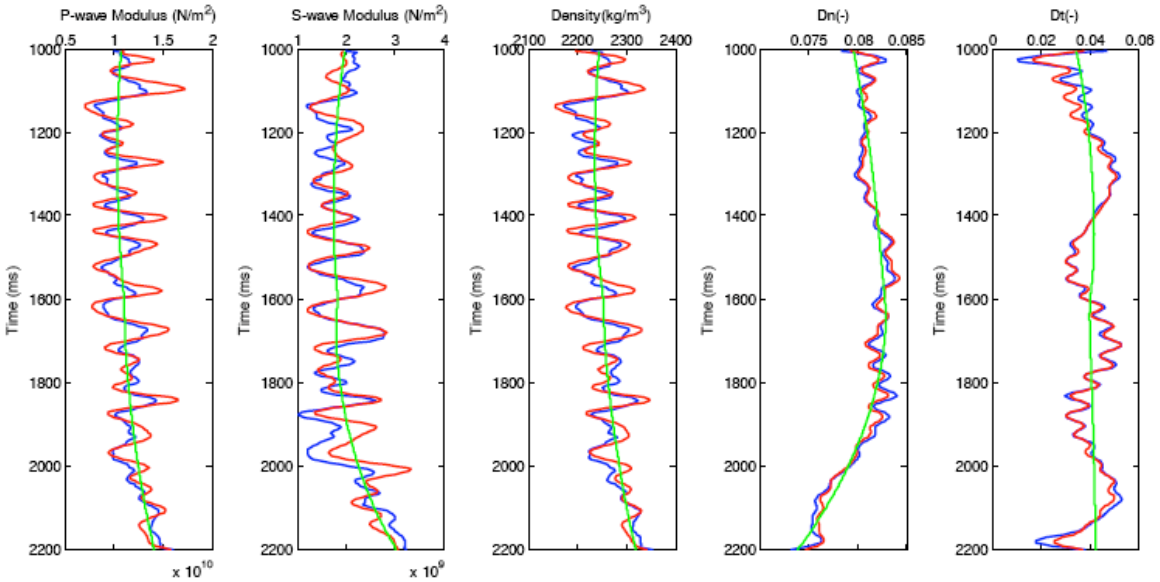

Figure 1: Real model (blue), initial model (green) and inverted result (red) for a model test without noise.

decomposition (SVD) damping optimization method, we can estimate the P-wave modulus, S-wave modulus, density, normal weakness and tangential weakness, respectively.

5. SYNTHETIC TEST

We test the proposed azimuthal simultaneous elastic inversion method on a synthetic earth profile from real well logs. We utilized the equation (12) incorporating the influence of seismic wavelets as forward solver to simulate the synthetic seismic data. Figure **1** displays the original (in blue), initial (in green) and inverted (in red) P-wave modulus, S-wave modulus, density, normal weakness and tangential weakness of known well with no noise in synthetic seismic data. The initial models are obtained by smoothing the original models. From Figure **1**, we see that all the parameters can be inverted well when there is no noise in the synthetic data even with very smooth initial model. Constraint from initial model enhances the stability of inversion. Figure **2** displays the original (in blue), initial (in green) and inverted (in red) P-wave modulus, S-wave modulus, density, normal weakness and tangential weakness of known well with 20% Gaussian noise in synthetic seismic data. From the inversion results in Figure **2**, the parameters can still be estimated reasonably with 20% Gaussian noise in synthetic seismic data, which verifies the stability of the proposed method.

6. REAL DATA EXAMPLE

Full azimuth real data is utilized to validate the application of the proposed AVAZ inversion method. Six azimuthal stacked and three partial angle stacked seismic data for each azimuth are utilized in inversion. The inversion results of real data with proposed method are displayed from Figure **3** to Figure **7**. A fractured shale oil reservoir develops in the intersection. We can see that the weaknesses show anomalously high value at around CDP number 80 and samples 290 in the target reservoir. The estimated results with the proposed approach in this paper shows good agreement with drilling results.

7. CONCLUSIONS

In this paper, we parameterized the heterogeneous HTI medium with P-wave modulus, S-wave modulus, density, normal weakness and tangential weakness. Incorporating Born approximation with stationary phase approximation, the seismic scattering coefficient of heterogeneous HTI medium is further yielded in terms of P-wave modulus, S-wave modulus, density, normal weakness and tangential weakness. A practical AVAZ inversion approach with model constraint in Bayesian scheme is proposed to implement the estimation of the parameters. The introduction of prior information and model constraint enhance the stability of the inversion. Real data example shows that the estimated elastic

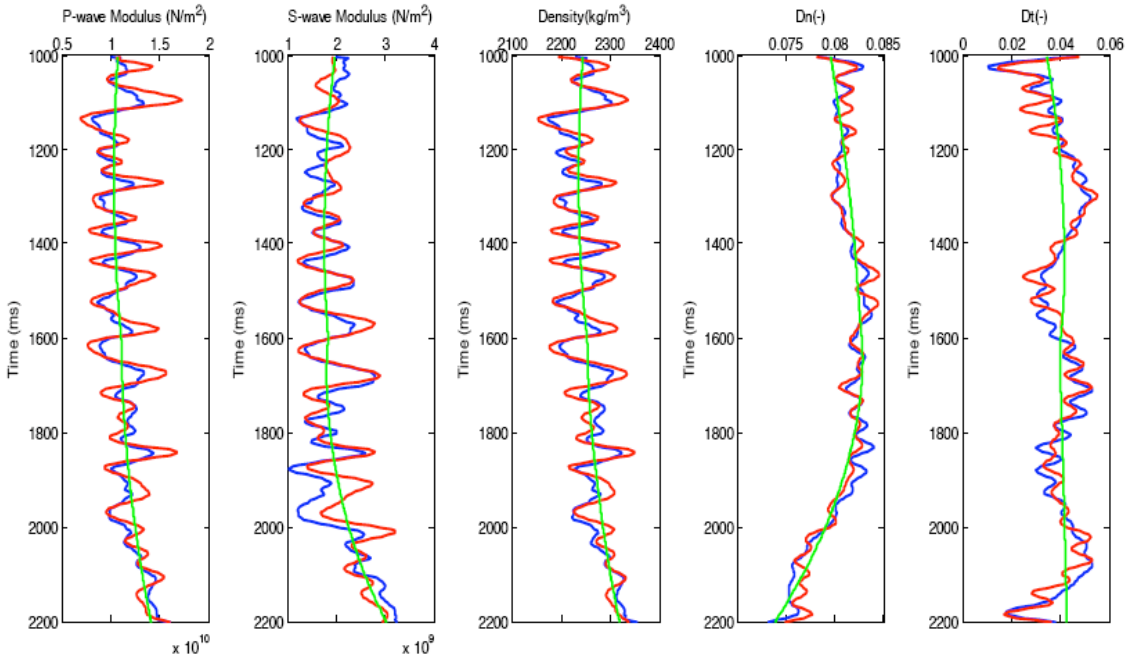

Figure 2: Real model (blue), initial model (green) and inverted result (red) for a model test with 20% noise.

modulus and fracture weakness may be helpful in evaluating the fractured shale oil/gas plays.

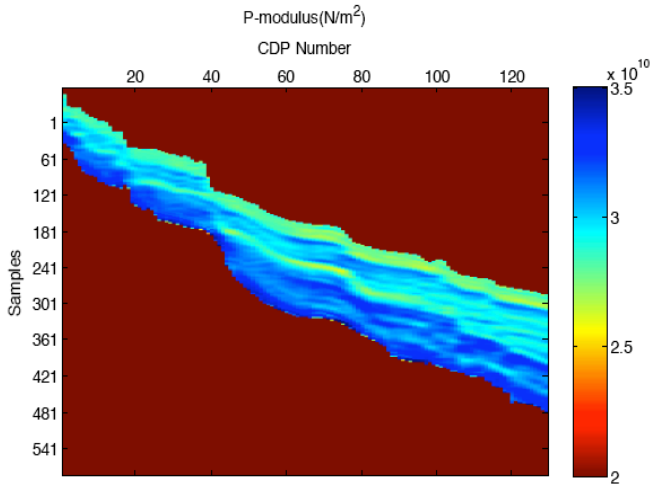

Figure 3: Inversion results of P-wave modulus.

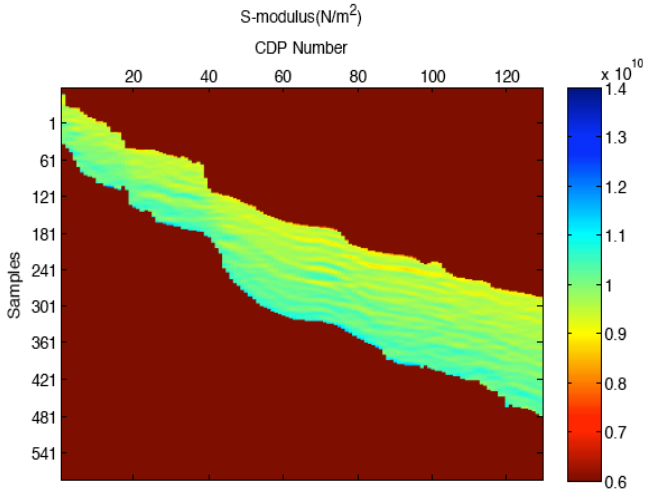

Figure 4: Inversion results of S-wave modulus.

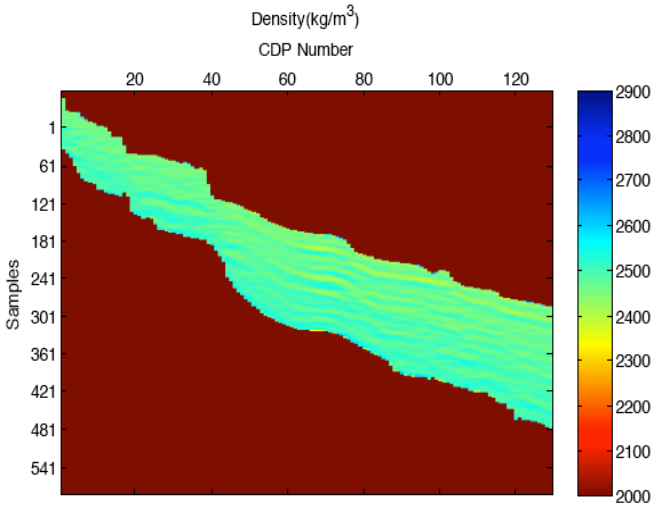

Figure 5: Inversion results of Density.

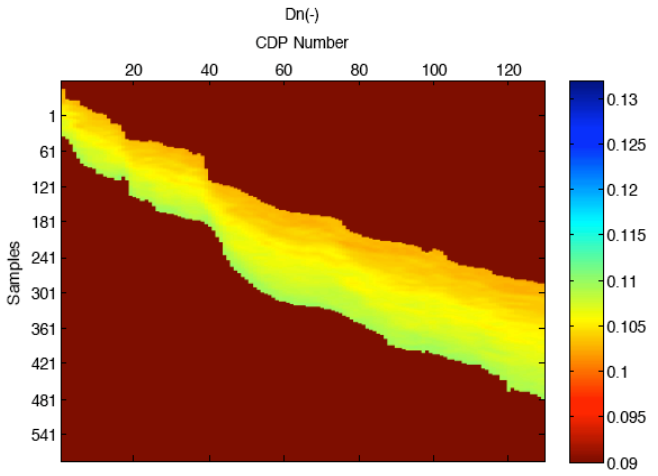

Figure 6: Inversion results of normal weakness.

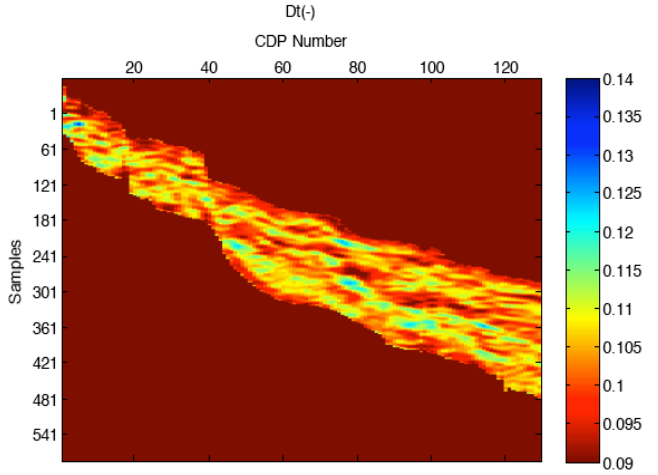

Figure 7: Inversion results of tangential weakness.

ACKNOWLEDGEMENTS

We would like to acknowledge the sponsorship of the National 973 Program of China (2013CB228604), China Postdoctoral Science Foundation (2014M550379), Natural Science Foundation of Shandong (2014BSE28009), Science Foundation for Post-doctoral Scientists of Shandong (201401018), Science Foundation for Post-doctoral Scientists of Qingdao and Science Foundation from SINOPEC Key Laboratory of Geophysics (33550006-14-FW2099-0038). The first author acknowledges the support of the Australian and Western Australian Governments and the North West Shelf Joint Venture Partners, as well as the Western Australian Energy Research Alliance (WA: ERA).

REFERENCES

[1] Schoenberg M. Elastic wave behavior across linear slip interfaces. The J Acoust Soc Am 1980; 68(5): 1516-1521. http://dx.doi.org/10.1121/1.385077

[2] Hudson J. Overall properties of a cracked solid. Cambridge Univ Press 1980; 88(2): 371-384.

[3] Hudson J. Wave speeds and attenuation of elastic waves in material containing cracks. Geophy J Royal Astron Soc 1981; 64(1): 133-150. http://dx.doi.org/10.1111/j.1365-246X.1981.tb02662.x

[4] Thomsen L. Weak elastic anisotropy. Geophysics 1986; 51(10): 1954-1966. http://dx.doi.org/10.1190/1.1442051

[5] Bakulin A, Grechka V, Tsvankin I. Estimation of fracture parameters from reflection seismic data-Part I: HTI model due to a single fracture set. Geophysics 2000; 65(6): 1788-1802. http://dx.doi.org/10.1190/1.1444863

[6] Corrigan D, Withers R, Darnall J, Skopinski T. Fracture mapping from azimuthal velocity analysis using 3-D surface seismic data. SEG Technical Program Expanded Abstracts 1996; 1834-1837.

[7] Tsvankin I. Anisotropic parameters and P-wave velocity for orthorhombic media. Geophysics 1997; 62(4): 1292-1309. http://dx.doi.org/10.1190/1.1444231

[8] Grechka V, Tsvankin I. 3-D description of normal moveout in anisotropic inhomogeneous media. Geophysics 1998; 63(3): 1079-1092. http://dx.doi.org/10.1190/1.1444386

[9] Grechka V, Tsvankin I, Lai Zhongkang. 3-D moveout inversion in azimuthally anisotropic media with lateral velocity variation; theory and a case study. Geophysics 1999; 64(4): 1202-1218. http://dx.doi.org/10.1190/1.1444627

[10] Lynn H, Beckham W, Simon K, Bates C, Layman M, Jones M. P-wave and S-wave azimuthal anisotropy at a naturally fractured gas reservoir, Bluebell-Altamont Field, Utah. Geophysics 1999; 64(4): 1312-1328. http://dx.doi.org/10.1190/1.1444636

[11] Jenner E. Azimuthal anisotropy of 3-D compressional wave seismic data, Weyburn field, Saskatchewan. Canada, Colorado School of Mines 2001.

[12] Ruger A. P-wave reflection coefficients for transversely isotropic models with vertical and horizontal axis of symmetry. Geophysics 1997; 62(3): 713-722. http://dx.doi.org/10.1190/1.1444181

[13] Sayers CM, Rickett JE. Azimuthal variation in AVO response for fractured gas sands. Geophy Prosp 1997; 45(1): 165-182. http://dx.doi.org/10.1046/j.1365-2478.1997.3180238.x

[14] Ruger A. Variation of P-wave reflectivity with offset and azimuth in anisotropic media. Geophysics 1998; 63(3): 935-947. http://dx.doi.org/10.1190/1.1444405

[15] MacBeth C. Azimuthal variation in P-wave signatures due to fluid flow. Geophysics 1999; 64(4): 1181-1192. http://dx.doi.org/10.1190/1.1444625

[16] Gray D, Roberts G, Head K. Recent advances in determination of fracture strike and crack density from P-wave seismic data. The Leading Edge 2002; 21(3): 280-285. http://dx.doi.org/10.1190/1.1463778

[17] Hall SA, Kendall JM, Barkved OI. Fractured reservoir characterization using P-wave AVOA analysis of 3D OBC data. The Leading Edge 2002; 21(8): 777-781.

[18] Zhu P, Wang J, Yu W, Zhu G. Inverting reservoir crack density from P-wave AVOA data: Journal of Geophysics and Engineering 2004; 1(2): 168. http://dx.doi.org/10.1088/1742-2132/1/2/010

[19] Chen H, Brown RL, Castagna JP. AVO for one- and two-fracture set models. Geophysics 2005; 70(2): C1-C5. http://dx.doi.org/10.1190/1.1884825

[20] Downton J, Russell H. Azimuthal fourier coefficients: A simple method to estimate fracture parameters. SEG Technical Program Expanded Abstracts 2011; 269-273.

[21] Xu Y, Li X, Dai H. Azimuthal AVO and seismic scattering attenuation in 3D fractured media: a numerical simulation study on the Discrete Fracture Model. SEG Technical Program Expanded Abstracts 2010; 483-487.

[22] Chen H, Zhang G, Yin X. AVAZ inversion for elastic parameter and fracture fluid factor. SEG Technical Program Expanded Abstracts 2012; 1-5.

[23] Sil S, Davidson M, Zhou C, Olson R, Swan H, Howell J, Chiu S *et al*. Effect of near-surface anisotropy on a deep anisotropic target layer. SEG Technical Program Expanded Abstracts 2011; 305-309.

[24] Far M, Thomsen L, Sayers C. Seismic characterization of reservoirs with asymmetric fractures. Geophysics 2013; 78(2): N1-N10.

[25] Fryer GJ, Frazer LN. Seismic waves in stratified anisotropic media. Geophy J Royal Astron Soc 1984; 78(3): 691-710. http://dx.doi.org/10.1111/j.1365-246X.1984.tb05065.x

[26] Thomsen L. Elastic anisotropy due to aligned cracks in porous rock. Geophy Prosp 1995; 43(6): 805-829. http://dx.doi.org/10.1111/j.1365-2478.1995.tb00282.x

[27] Aki K, Richards PG. Quantitative seismology. vol. 1: NY: WH Freeman and Company 1980.

[28] Jech J, Pšenčik I. First-order perturbation method for anisotropic media. Geophys J Int 1989; 99(2): 369-376. http://dx.doi.org/10.1111/j.1365-246X.1989.tb01694.x

[29] Shaw RK, Sen MK. Born integral, stationary phase and linearized reflection coefficients in weak anisotropic media. Geophys J Int 2004; 158(1): 225-238. http://dx.doi.org/10.1111/j.1365-246X.2004.02283.x

[30] Shaw RK, Sen MK. Use of AVOA data to estimate fluid indicator in a vertically fractured medium. Geophysics 2006; 71(3): C15-C24.

[31] Cerveny V, Berryman J. Seismic ray theory. Appl Mech Rev 2002; 55(6): B118-B119.

[32] Zong Z, Yin X, Wu G. AVO inversion and poroelasticity with P- and S-wave moduli. Geophysics 2012; 77(6): N17-N24. http://dx.doi.org/10.1190/geo2011-0214.1

[33] Zong Z, Yin X, Wu G. Elastic impedance variation with angle inversion for elastic parameters. Journal of Geophysics and Engineering 2013; 9(3): 247-260. http://dx.doi.org/10.1088/1742-2132/9/3/247

[34] Zong Z, Yin X, Wu G. Direct inversion for a fluid factor and its application in heterogeneous reservoirs. Geophy Prosp 2013; 61(5): 998-1005. http://dx.doi.org/10.1111/1365-2478.12038

[35] Zong Z, Yin X, Wu G. Elastic impedance parameterization and inversion with Young's modulus and Poisson's ratio. Geophysics 2013; 78(6): N35-N42. http://dx.doi.org/10.1190/geo2012-0529.1

Received on 19-11-2014 Accepted on 29-11-2014 Published on 08-01-2015

DOI: http://dx.doi.org/10.15377/2409-787X.2014.01.02.3